Arch Dermatol Res (2011) 303:457–473
DOI 10.1007/s00403-011-1152-x

REVIEW ARTICLE

Optical coherence tomography in dermatology: technical and clinical aspects

Thilo Gambichler · Volker Jaedicke · Sarah Terras

Received: 5 February 2011 / Revised: 4 May 2011 / Accepted: 19 May 2011 / Published online: 7 June 2011

Abstract Optical coherence tomography (OCT), a fairly new non-invasive optical real-time imaging modality, is an emergent in vivo technique, based on the interference (Michelson interferometry) of infrared radiation and living tissues, that allows high-resolution, 2- or 3-dimensional, cross-sectional visualisation of microstructural morphology of tissues. OCT provides depth-resolved images of tissues with resolution up to a few micrometers and depth up to several millimetres depending on tissue type. The investigations using OCT to assess skin structure in clinical settings started in the past decade and consequently proved that this imaging method is useful in visualizing subsurface structures of normal skin, including the epidermis, dermoepidermal junction, dermis, hair follicles, blood vessels and sweat ducts. An increasing number of papers brought evidence of the utility and the precision of OCT technology, in its different technical variants, in diagnosing and monitoring skin disorders, including malignancies and inflammatory conditions, respectively. The present comprehensive review describes and illustrates technical aspects and clinical applications of OCT methods in dermatology.

T. Gambichler (✉) · S. Terras
Department of Dermatology, Ruhr-University Bochum, Gudrunstr. 56, 44791 Bochum, Germany
e-mail: t.gambichler@klinikum-bochum.de

S. Terras
e-mail: s.terras@klinikum-bochum.de

V. Jaedicke
Photonics and Terahertz Technology, Ruhr-University Bochum, Universitätsstr. 150, 44780 Bochum, Germany
e-mail: volker.jaedicke@rub.de

Keywords Optical coherence tomography · Dermatology · Skin imaging · Interferometry · Histology

Historical aspects of OCT

In the past decade optical coherence tomography (OCT) has developed from a promising optical biomedical imaging technique to a standard method in some medical fields. OCT is a non-invasive imaging technique that allows real-time cross-sectional evaluation of biological tissues, e.g. skin. OCT is based on low-coherence interferometry (LCI) to produce depth profiles, which are equivalent to the ultrasound A-Scans. This A-Scan technique has been developed at the University of Essen [23, 25] and used for eye length measurements. First 2D structure B-Scan images have been shown at the ICO-15 conference in 1990 [21]. This concept has been picked up by other groups and was further developed through collaboration between the New England Eye Center, Tufts University School of Medicine, the Department of Electrical Engineering and Computer Science at Massachusetts Institute of Technology, and Lincoln Laboratory, Massachusetts Institute of Technology. In 1991, Huang et al. [48] published the first in vitro tomogram of the human eye. The first in vivo medical image has been presented by Fercher et al. in 1993 [24]. The introduction of OCT in ophthalmology led to advanced diagnostic capabilities. Since then, clinical and experimental applications of OCT have exponentially been developed in medicine. Meanwhile, OCT is used in many domains of medicine: cardiology, gastroenterology, urology, surgery, neurology, rheumatology, pneumology, gynaecology and dentistry for both research and clinical practice [9, 13, 17, 28, 61, 92, 99, 101].

In 1997, OCT has been introduced in dermatology, and it is now being increasingly employed in clinical skin research [111]. With OCT, the stratum corneum of glabrous skin (palmoplantar), the epidermis and the upper dermis can clearly be identified. Moreover, skin appendages and blood vessels can be visualized. Histology still represents the gold standard for micro-morphological investigation. Nevertheless, skin biopsy is traumatic and cannot be repeated on identical skin sites. Hence, diagnosis and monitoring of skin changes by means of non-invasive imaging techniques may potentially enrich dermatologic research and practice [4, 36, 37, 124]. Some OCT scanners for dermatological purposes are already available on a commercial basis (e.g. Michelson Diagnostics, Kent, United Kingdom; IMALUX, Cleveland, OH, USA, Bioptigen, Durham, North Carolina, USA; Thorlabs, Newton, NJ, USA). All OCT images included in this review have been captured with a SkinDex 300 (ISIS optronics GmbH, Mannheim, Germany). The OCT measurements have been conducted using a contact glass and index matching gel. More technical details on the SkinDex 300 can be found in previous papers [58, 60].

OCT technology

Principles and operation

The principle of OCT imaging is analogous to that of ultrasound imaging. OCT measures echo delays and the intensity of back-reflected infrared light rather than acoustic waves. In contrast to ultrasound OCT does not require a direct contact between device and sample. As the velocity of light is extremely high, direct measurement of optical echoes cannot be performed electronically as in ultrasound. Thus, OCT is based on LCI. In LCI, light backscattered from inside the specimen is measured by correlating it with light that has travelled a known reference path. Only ballistic and near-ballistic, sparse scattered photons carry the depth information. The diffuse background of multiple scattered photons has to be filtered out. The most part of these multiple scattered photons, which do not carry any depth information, can be filtered out by the so-called coherence gate. When the path length of the multiple scattered photons is smaller than the coherence length they also contribute to the OCT image and degrade the contrast and the resolution [91].

The centre wavelength of the light source determines the maximum penetration depth of the OCT system through the optical properties of the tissue and wavelength dependence of these properties. For OCT, the system's wavelength has to be such that absorption and scattering in the sample is minimised to allow maximal imaging depth. In tissue, absorption is minimised between 700 and 1,300 nm, in what is known as the window of transmission [105]. In general, the scattering decreases in the form of an inverse power law; thus larger wavelengths are better suited for imaging deeper structures [84].

In OCT, in contrast to a pure confocal design, the axial and lateral resolution is not coupled. The source coherence length and the spot size of the beam focus on the sample determine the depth resolution and lateral image resolution, respectively. Systems with ultrahigh depth resolution of about 1 μm have been developed [107]. Nevertheless, depth resolution on the order of 5–10 μm is more common [3].

In OCT incident light is backscattered from the internal structure that is being imaged. When the light propagates through the tissue it is strongly attenuated by wavelength-dependent scattering and wavelength-dependent absorption. In skin tissue, scattering is predominant over absorption. The backscattering is proportional to the second-order derivative of the scattering potential, which depends on the first and second derivatives of the sample refractive index [22]. Contrast in standard OCT thus mainly originates from the change of the refractive index. Only the ballistic photons backscattered to the OCT system contribute to the OCT image; therefore, by analyzing the exponential profile of light attenuation detected by the OCT system, one can obtain information on tissue scattering properties. The so-called anisotropy coefficient is the cosine of the mean scattering angle. It plays an important role in OCT as it determines the amount of backscattered and multiple scattered light [58].

With regard to the impact on scattering alterations of distribution, size, density and orientation of particles are of higher importance than the content of pigment, for example. To obtain maximum penetration depth longer wavelengths around 1,300 nm are suitable, while for a better image contrast central wavelengths around 800 nm are more appropriate [3].

OCT imaging modalities split up into various concepts. The most important techniques are OCT in the time domain (TD-OCT) and in the frequency domain (FD-OCT).

The principal OCT system design is an interferometer. One interferometer arm contains a modular probe that focuses and scans the light onto the sample. The second interferometer arm is the so-called reference path that is equipped with a mirror. In the next paragraphs the most common imaging modalities will be described.

Time domain OCT (TD-OCT)

In TD-OCT the reference arm is equipped with a translating mirror or scanning delay line. Fig. 1 shows a typical TD-OCT system.

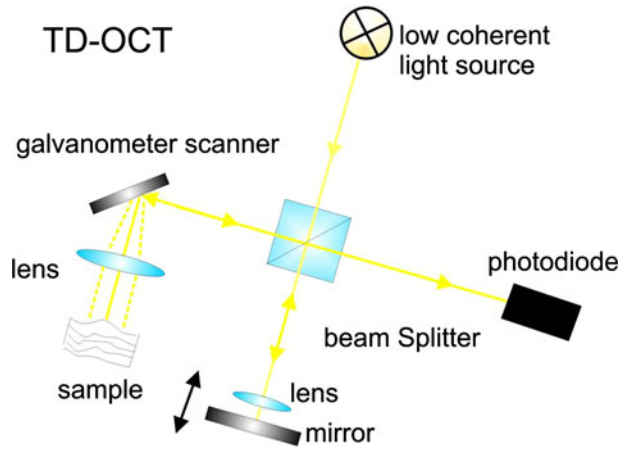

Fig. 1 Time domain OCT system, A-Scans are obtained by moving the mirror in the reference arm

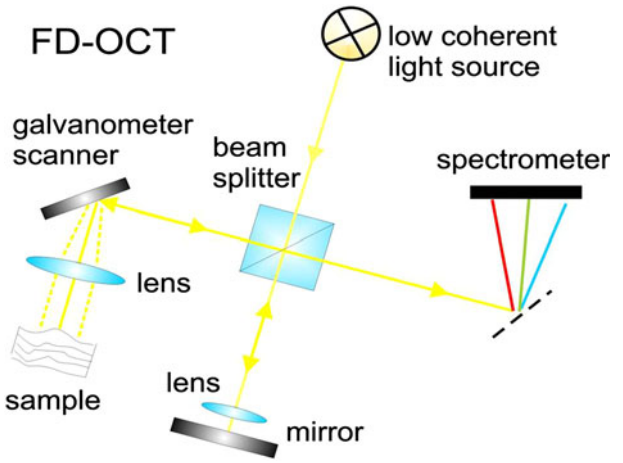

Fig. 2 Frequency domain OCT system, A-Scans are obtained when the spectra, which are recorded by the spectrometer, are fourier transformed

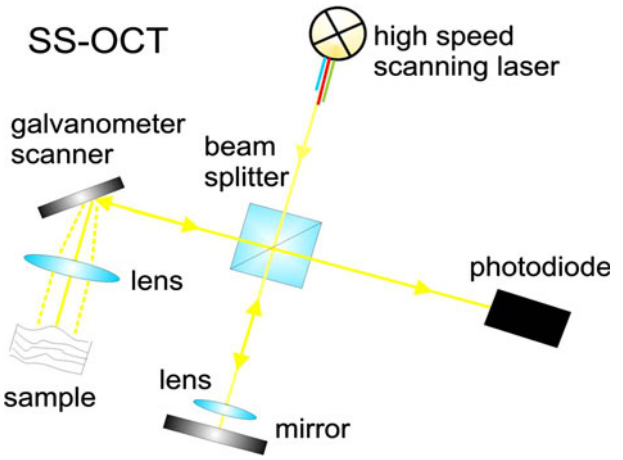

Fig. 3 Swept source OCT system. An A-Scans is recorded when the laser scans over the wavelength range and the recorded spectrum is fourier transformed

The coherence length of light determines the distance between two points in space where interference is possible. Thus, when the distance between the reference arm and the point inside the tissue, where the backscattering takes place is longer than the coherence length, no interference fringes on the detector are observed. Thus, depth filtering can be performed by this coherence gate which restricts the imaged area to the coherence length. To image the internal tissue structure as a function of depth, the mirror in the reference arm is shifted periodically and the time-dependent signal is recorded. The detected interference fringes are demodulated and form the A-Scan. Cross-sectional images are recorded when several A-Scans from different positions are combined. To achieve high resolution over the whole imaging depth, the lens that focuses the light into the sample can be moved with the reference mirror simultaneously. Hence, the coherence and focal gate is matched across the whole scanning depth.

Frequency domain OCT (FD-OCT)

There are two main approaches in FD-OCT and in both the mirror in the reference arm is fixed. In the first approach the detector is replaced by a spectrometer. A typical FD-OCT system is shown in Fig. 2. The axial depth scan can be performed without mechanical movement by reading out the diode array of the spectrometer. The light that is backscattered from different depths in the tissue and superimposes with the light from the reference arm, modulates the spectra. The modulation frequency is directly proportional to the depth of the tissue structures. Hence, a Fourier transform of the spectra gives direct access to the depth information.

The second approach is called swept source OCT (SS-OCT). SS-OCT systems are working with a similar principle, which is shown in Fig. 3. Here, the broad band white light source is replaced by a light source that scans the wavelengths of the spectrum over a time interval. Thus, the spectrometer can be replaced by a simple photo diode, which allows high-speed detection. An A-Scan is recorded by the detector when the laser is scanning over one wavelength interval. The recorded data are equivalent to the data recorded by the spectrometer. Thus, a Fourier transform gives access to the depth information.

Several studies outlined the higher sensitivity and faster image acquisition of FD-OCT systems in comparison with TD-OCT systems [12, 15, 63]. Typical fast 50 kHz SS-OCT systems record 3-dimensional data sets in approximately 1 s, while recent publications reported line scan rates of 20 million A-Scans per second [116]. Although TD-OCT systems still have these disadvantages, there is an inherent advantage to FD-OCT. In FD-OCT the focus

position in the sample is fixed since the signal over the depth is recorded at once. Thus, a dynamic focus which enables a constant spot size over depth is not possible. To overcome this problem multi-beam OCT systems have been developed. In this approach a set of beams is scanned across the sample simultaneously [47]. Each beam is focused at a different depth. Hence, a combination of all beams gives access to images with high lateral resolution.

Functional OCT

In this paragraph several technologies are described which analyze different physical parameters of the backscattered light. This additional information can be valuable for diagnostic purposes. As described above, image contrast in standard OCT is mainly produced by the variation of the diffractive index inside the tissue. Nevertheless, any physical property that changes the amplitude, phase, or polarization of the light which propagates through the tissue can be used to extract information of diagnostic value.

Polarization-sensitive OCT (PS-OCT) has the ability to visualize and quantify the birefringence properties of skin [20, 67, 69, 71, 79, 85, 89, 97] and thus has been used as an efficient tool for tissue segmentation [43]. Many types of tissue are distinguishable in PS-OCT, in particular those with a significant collagen content such as the skin. Loss of collagen structure and integrity is often associated with abnormalities of the skin, including tumours and connective tissue diseases. This suggests that birefringence assessments may prove valuable as a diagnostic indicator of certain cutaneous pathologies.

Optical Doppler tomography (ODT), which is also called Doppler OCT, exploits the Doppler frequency shift. This frequency shift is introduced when objects inside the sample, for example blood, is moving. In FD-OCT, the most common approach to measure flow velocities is called phase-resolved Doppler OCT. In this method the phase change between sequential A-Scans is analyzed to calculate spatially resolved velocity profiles. The velocity profiles can reach sub-mm/s velocity sensitivity with real-time acquisition rates. Measurements in depths of around 1.0 mm have been achieved. Applications of this technique for monitoring changes in blood flow dynamics and vessel structure following pharmacological intervention and photodynamic therapy have been demonstrated [1, 10, 49, 64, 75, 102, 106, 121, 123].

Spectroscopic OCT (S-OCT) is another area of investigation. In all techniques that use reflected and backscattered light for imaging of tissue, the specific absorption and scattering properties of the intermediate tissues determine the spectral properties of light that is detected from each location within the tissue. S-OCT is used to enhance image contrast and makes it possible to differentiate tissue pathologies by their spectroscopic properties or functional state. S-OCT might thus serve as a type of 'spectroscopic staining', analogous to staining in histology, and it has the potential to detect spatially resolved functional and biochemical tissue information over the entire region of emission wavelength of the light source with a single measurement [18]. In S-OCT there are two main approaches; one approach uses OCT systems with multiple wavelength bands, while in the other time-frequency distributions are applied in a post processing manner. For each of this wavelength bands, typically two, an image is recorded [14, 80, 83, 95]. These images can be combined in a differential manner, giving access to spectroscopic information. The method benefits of the high-resolution cross sectional images and the huge bandwidth, but suffers of the high complexity of the systems and the poor spectral resolution.

As mentioned above spectral information can also be obtained in a post processing procedure by using time–frequency distributions. These can be applied in the time (spatial) domain [53, 72] or frequency (wave number) [65] domain. The most common algorithm is the short-time Fourier transform (STFT), followed by wavelets and spectral estimation techniques [52, 81, 118]. Several studies differentiated oxygenation states of blood by Spectroscopic OCT [19, 82]. Other groups utilised the correlation between scatter size and spectral modulations [44, 52]. Combined with pattern recognition techniques these made the differentiation of tissue types with the help of scatter size, e.g. nucleus size, possible [52].

The sensitivity of OCT to displacement of living tissue during imaging is a troublesome issue that can lead to undesired blurring of images. OCT elastography takes advantage of this sensitivity to quantify microscopic deformations inside tissue induced by externally applied stress. The aim of OCT elastography or elacticity imaging is to assess the local variations of the stiffness inside a tissue non-invasively. The primary quantitative measure of the stiffness is the shear elastic modulus which varies widely for different types of tissues. A number of pathological processes, including oedema, fibrosis and calcification, may alter the elastic modulus of the extracellular tissue matrix. Possible dermatological applications of OCT elastography include, for example, differentiation of hard and soft masses during tissue biopsy and evaluation of wound healing in vivo [54, 90].

The integration of nonlinear optical contrasts in OCT systems is a promising approach to achieve resolution on cellular level and biochemical specificity. OCT has been combined with several other imaging modalities like multiphoton microscopy (MPM) which exploit fluorescent or other physical processes. It has been shown that the combination of OCT and MPM provides a powerful tool for skin cancer diagnosis and other skin diseases [59, 98, 117].

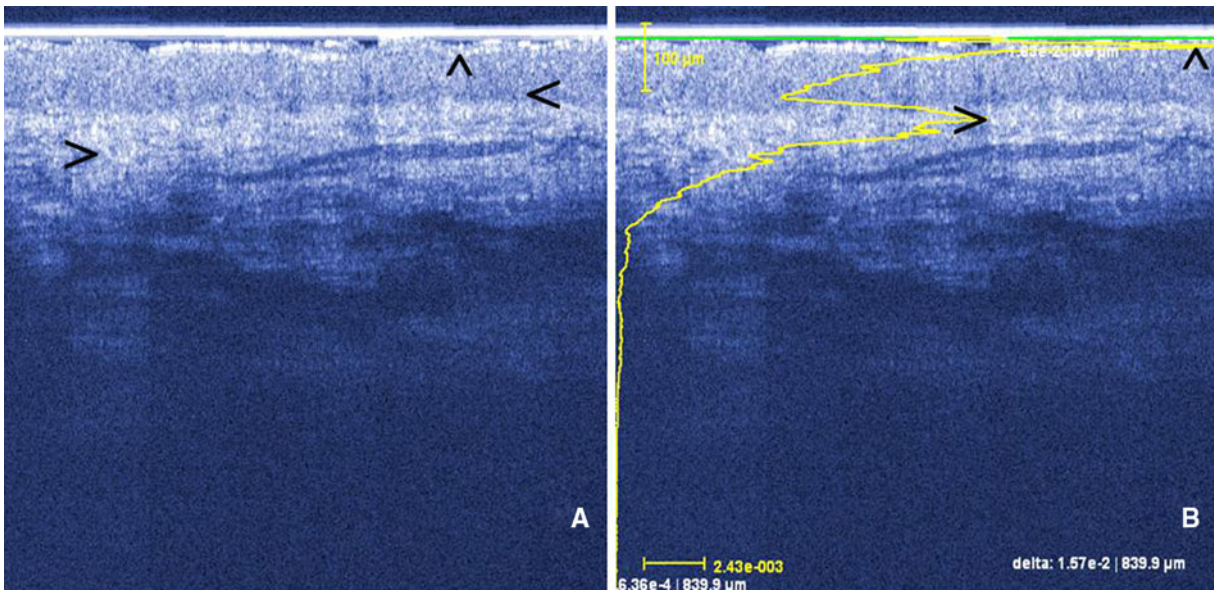

Fig. 4 OCT image (B-scan) of normal human skin on the upper back showing a thin hyperreflective band (*cap symbol* entrance echo), the epidermis border (*less than symbol*) and demarcation of the dermo-epidermal junction zone, hyperreflectivity (collagen bundles *greater than symbol*) and long cavities (vessels) in the upper dermis (**a**). In addition (**b**), the A-scan of human skin is shown (*cap symbol* entrance peak, *greater than symbol* second intensity peak)

Appearance of normal skin on OCT

In order to correctly interpret skin pathologies in OCT images, the appearance of healthy skin has to be studied at first (Fig. 4).

Stratum corneum

Usually, the stratum corneum or horny layer is only visible in skin on the palms and soles since in other anatomic sites the stratum corneum is not thick enough to be visible at the resolution of conventional OCT technique. The dermatoglyphics (fingerprint patterns) in palmoplantar skin create a wavy surface on OCT images. The stratum corneum can be seen as a dense, well-defined, homogenous, low-scattering band, occasionally with some high-scattering sweat gland ducts inside. The average thickness of the stratum corneum on the fingertips is about 300 µm as measured by OCT in vivo (Fig. 5) [27, 41, 109, 111, 113].

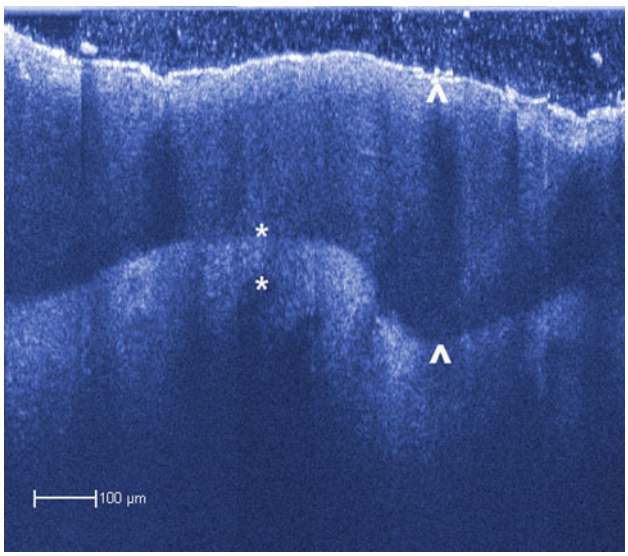

Fig. 5 OCT image showing the stratum corneum (*arrows*) and epidermis (*asterisk*) of a fingertip

Epidermis

The epidermis of the face and body is the first distinguishable layer in the OCT image, except for palms and soles (see above). The epidermis shows less intense signals than the dermis and can be distinguished from the upper corium if the border is relatively flat and not too ridged. Epidermal thickness can easily be measured using the averaged A-Scan [109–111, 115]. The most commonly used method for the assessment of the epidermal thickness is measuring the distance between the first intensity peak (also called entrance peak) and the second intensity peak in the averaged A-Scan [29, 111]. However, studies indicate that the valley before the second peak most likely corresponds to the dermo-epidermal junction—thus, the entrance peak and the valley before the second peak most probably delineate the epidermis thickness. The second peak in the A-Scan is very likely caused by the backscattering of light at the fibrous structure of collagen in the dermis. Taking this into consideration, it can be stated that

peak-to-peak measurements probably overestimate epidermal thickness as confirmed in several correlation studies [29, 30, 74]. Another possibility to measure epidermal thickness is using a B-scan with an integrated measuring tool (ruler) to measure the distance from the skin surface reflection (entrance signal) to the first well-demarcated change of reflectivity with clear signal-poor zones [29, 37]. Weissman et al. [108] described another, more complicated method for measuring epidermal thickness [108]. They used a shapelet-based image processing technique that automatically identifies the upper and lower boundaries of the epidermis and measures its thickness in vivo [108]. Epidermal thickness as measured with OCT was found to decrease with age, independent of gender, body localisation and skin-type [35, 69]. Only forehead skin was shown to be significantly thinner in old females when compared with that in old men [35]. Recently, Josse et al. [51] reported on a new image processing method for measuring ET from OCT images that significantly reduces calculation time for this parameter and avoids user intervention. The main advantages of this automatic measurement are that data can be analyzed more rapidly and reproducibly in clinical trials.

Dermis

The dermis is usually more signal intense than the epidermis with some signal-poor cavities corresponding to blood vessels. Dermal signal intensity on OCT can predominantly be ascribed to the extracellular matrix, in particular the collagen fibre network.

Skin appendages

Hair follicles and ducts of sebaceous glands can be seen as lower reflecting regions within the intensely reflecting epidermis [109].

Clinical applications of OCT in dermatology

Psoriasis

Psoriasis is a chronic inflammatory skin disease, histopathologically characterized by hyperkeratosis, parakeratosis, acanthosis, Munro's micro abscesses and elongation of the rete ridge (papillomatosis). Inflammatory cell infiltration can be observed in the upper dermis. On OCT images of psoriatic patches, the regional parakeratosis is seen as a strong entrance signal, sometimes composed of several parallel layers [110]. This layered image arises because of the poorly backscattering region that corresponds to poorly differentiated cells at the background of mature highly backscattering keratinocytes. In a hyperkeratotic condition such as psoriasis, the backscattering from the thickened horny layer is higher than that from cellular layers. Therefore, the depth of the OCT imaging in psoriasis is reduced. However, keratin masses, in particular on non-glabrous skin as well, can be visualized. Psoriatic pustules are seen as intraepithelial holes with strongly scattering, signal-intense structures inside [110].

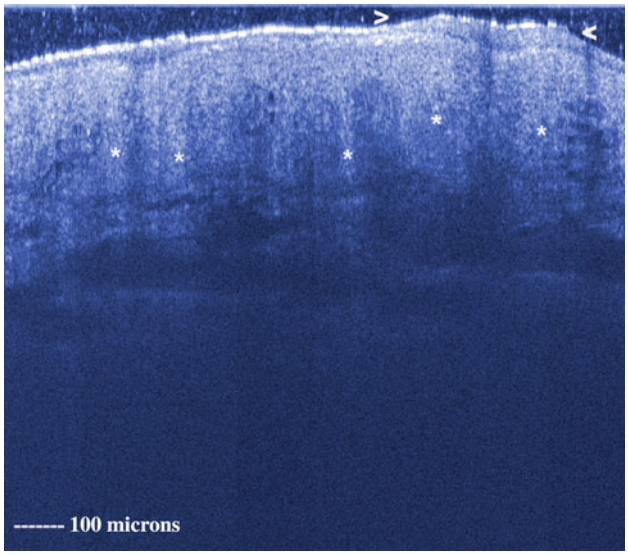

Fig. 6 OCT of psoriasis vulgaris showing a thickened hyperreflective band (*arrow heads* thickened stratum corneum) and acanthotic epidermis (*asterisk*) with elongated rete ridges

The acanthotic epidermis may be evaluated by thickness measurements by means of the B-Scan or averaged A-Scan. However, the second peak in the A-Scan is often difficult to detect due to the psoriasiform papillomatosis leading to a less defined border between epidermis and dermis. The signal attenuation of the psoriatic dermis is lower than in healthy skin, due to the perivascular inflammatory infiltrates. Also, dilated blood vessels can be visualised in OCT images of psoriatic skin [8, 109–111]. A recent study by Morsy et al. [73] suggests that OCT may be used to measure epidermal thickness in psoriasis and that these measurements correlate with several other parameters of disease severity. This implies that OCT assessment of psoriatic plaques may provide a useful method for non-invasive in vivo method to follow the evolution of psoriatic lesions (Fig. 6).

Contact dermatitis

Inflammatory skin diseases have already been extensively studied in vivo using OCT [41, 109–111]. Welzel et al. [110] demonstrated that the changes in skin due to inflammation are clearly visible in OCT images. For example, in irritant contact dermatitis larger and more irregular skin folds are seen on the skin surface. The

Table 1 Correlation of the histopathological findings and features on OCT images in cutaneous lupus erythematosus as described by Gambichler et al. [33]

Histopathologically	OCT
Marked hyperkeratosis	Thickening and disruption of entrance signal
Marked atrophy and flattening of the viable epidermis	Very thin and flattened layer below entrance signal
Dense patchy lymphocytic infiltrates and oedema in the upper dermis	Patchy reduction of reflectivity in the upper dermis
Dilated vessels in the upper dermis	Increased signal-free cavities in the upper dermis

entrance signal is frequently thickened and stronger. Epidermal thickening due to spongiosis and acanthosis can be seen, together with signal-free cavities corresponding to dilatation of blood vessels in the dermis. Spongiosis can be visualized as thin, poorly backscattering fissures at the background of the signal intense epidermis, whereas intercellular oedema leads to a decrease of backscattering from cellular layers [41]. Previously, we have investigated acute allergic contact dermatitis by means of OCT. The images of acute allergic contact dermatitis showed pronounced skin folds, thickened and/or disrupted entrance signals and a significant increase in epidermal thickness. Also, sharply demarcated signal-free cavities within the epidermis and a considerable reduction of dermal reflectivity could be seen. These aforementioned changes correlated strongly with the clinical patch test grading [38].

Lupus erythematosus

To our best knowledge, we were the first study group investigating the diagnostic value of OCT in chronic discoid lupus erythematosus (LE) and subacute cutaneous LE. We were able to demonstrate micromorphological changes of cutaneous LE that correlated with histopathological findings (Table 1). All OCT parameters studied significantly correlated with histopathological features as indicated by correlation coefficients ranging from 0.55 to 0.94. Hence, we suggest that OCT enables visualisation of micromorphological changes in cutaneous LE which correlate with histopathological findings. However, the OCT findings observed in this study are not specific enough to differentiate cutaneous LE from other inflammatory skin conditions. Nonetheless, OCT may be a promising method for objectively monitoring the activity of cutaneous lupus and the effects of treatment over time in vivo [33].

Blistering diseases

Intradermal or subepidermal blistering can easily be detected on OCT images as shown in Fig. 7 and by our previous study on allergic contact dermatitis [38]. Intraepidermal blisters can be distinguished from subepidermal blisters by looking for the location of the cleft at the lateral border of the blister. Besides the level of blisters its content can also

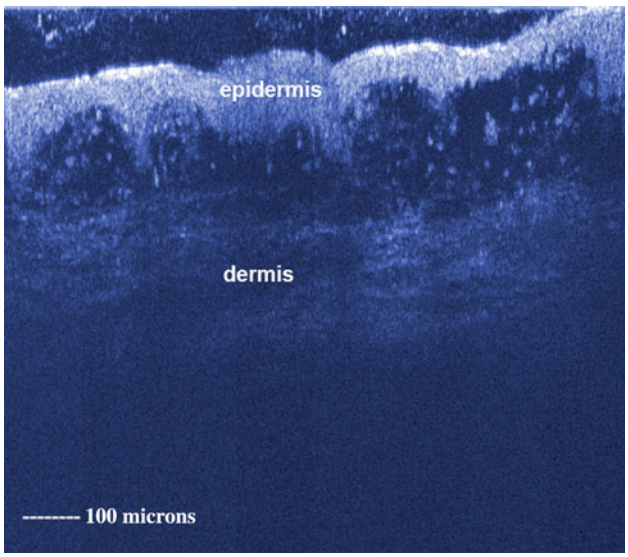

Fig. 7 OCT image of bullous pemphigoid showing a large cavity between the epidermis and dermis corresponding to blister formation

be determined by means of OCT in vivo. Serous fluid filling is poorly backscattering because of its high transparency and the small number of cellular elements, whereas pus contains a higher amount of cells and is therefore more backscattering [41, 62, 109, 111]. However, it is not possible to differentiate between pemphigoid lesions and pemphigus-like diseases such as subcorneal pustular dermatosis and Darier's disease because the variation is too subtle. This may be due to limited resolution, so enhanced resolution of OCT may overcome this obstacle [68].

Vascular skin lesions

OCT images can clearly distinguish dilated blood vessels or vascular abnormalities from normal tissue [10, 49, 75, 86, 100, 122]. With OCT, structural parameters of vascular lesions such as epidermal thickness and depth of the dilated blood vessels can be visualised. This information can be helpful in the selection of appropriate treatments [86]. It may even help to determine the photosensitizer dose and laser parameters in the photodynamic therapy for treatment of port wine stains [122]. The use of Doppler OCT may have the potential for identifying feeding vessels and

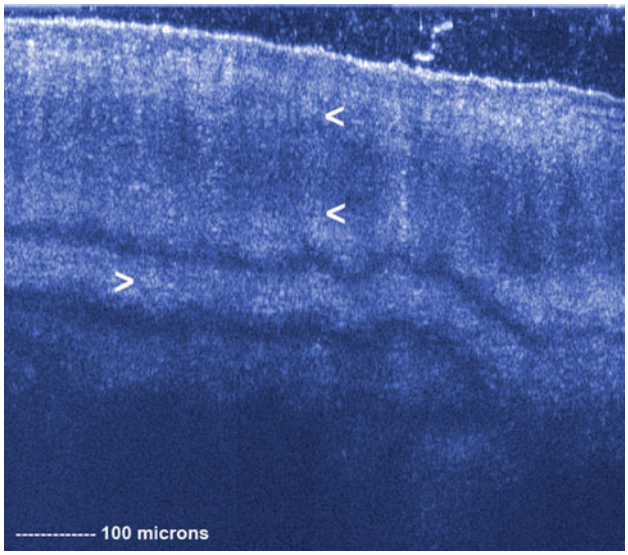

Fig. 8 OCT of a toe nail showing a well-demarcated nail plate and nail bed

prognosis estimation in capillary haemangiomas and vessels in general during laser treatment [71].

Infections and infestations

Beside the skin, finger and toe nails can also be assessed using OCT (Fig. 8). Onychomycosis is often difficult to clinically differentiate from other nail diseases such as psoriasis, lichen planus and dystrophic nail changes. With OCT imaging, fungal elements can be detected as highly scattering elongated structures inside the nail plate surrounded by areas of homogeneous decrease in signal intensity [2]. A pilot study by Abuzahra et al. [2] showed that OCT is a reliable, easy-to-use, non-invasive and non-destructive method to visualize fungal elements in onychomycosis in vivo. In previous studies, OCT also demonstrated potential for imaging of skin infestations such as larva migrans and scabies [71, 112].

Non-melanoma skin cancer

The term non-melanoma skin cancer predominantly comprises common skin tumours such as basal cell carcinoma (BCC), squamous cell carcinoma (SCC) and actinic keratosis (AK). For these tumours, OCT appears to be capable of visualizing the derivation of tumour cell aggregates from the epidermis.

Actinic keratosis

AK is an intraepithelial neoplasm divided into three grades characterized by partial-thickness epidermal dysplasia, hyperkeratosis, parakeratosis and solar elastosis. Approximately 10% of AK lesions will progress to SCC [42]. OCT images of AK show white dots and streaks corresponding to hyperkeratosis [50]. Barton et al. [6] suggested that OCT is useful for identifying and characterizing AK and monitoring their response to chemoprevention agents. Indeed, AK can be distinguished from non-diseased skin with 86% sensitivity and 83% specificity according to Korde et al. [60].

Basal cell carcinoma

Solid tumours are characterized by a homogenous signal distribution [26, 114]. In BCC, subepidermal hyperreflective zones can be seen in the OCT images, which had similar size, allocation and form as the tumour cell nests in histological sections. A narrow hyporeflective band separated the echo-rich tumour aggregates from the tumour stroma. Multiple smaller tumour cell nests in the deeper dermis were observed as echo poor roundish spots [7]. In a more systematic study we found that on OCT images of BCCs, a loss of normal skin architecture and a disarrangement of the epidermis and upper dermis were observed as compared with adjacent non-lesional skin. Furthermore, large plug-like signal-intense structures, honeycomb-like signal-free structures and prominent signal free cavities in the upper dermis were frequently detected. The latter features correlated with histology (Fig. 9) [39]. A pilot study by Olmedo et al. [76] also showed that an excellent correlation between OCT images and histopathological features of BCC can be established. Hence, OCT is capable of visualizing the altered skin architecture present in BCC, with good histopathological correlation. The same is true for polarization-sensitive OCT [97]. OCT was even found to be more precise and less biased than 20-MHz high-frequency ultrasound for thickness measurements in AK and BCC lesions <2 mm [70]. However, we have shown that it is not possible to differentiate between the different BCC subtypes (nodular, multifocal superficial and infiltrative) with OCT [39]. A study with observer-blinded evaluation of OCT images pointed out that AK and BCC cannot be discriminated based on the OCT images alone [50, 67]. Still, although OCT diagnosis is less accurate than clinical differential diagnosis, it has a relatively high accuracy in distinguishing lesions from normal skin and delineating tumour borders [67]. Moreover, machine-learning analysis suggests that when a multiplicity of features, extracted from the overall architecture of the OCT image, is used in combination a reasonable diagnostic accuracy for diagnosis of BCC and AK can be obtained [50]. Khandwala et al. [55] recently concluded that non-contact OCT imaging of the skin is a useful tool for demarcating BCCs on the face and eyelids. Moreover, Hamdoon et al. [45] demonstrated that OCT-guided photodynamic therapy is a promising approach to

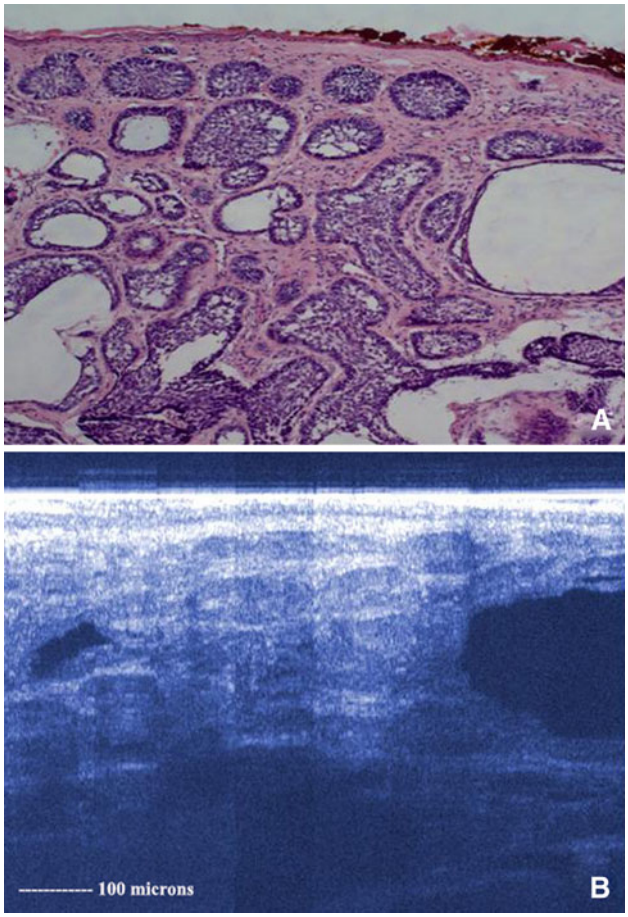

Fig. 9 Image (**a**) showing histology (hematoxylin–eosin) of an infiltrative basal cell carcinoma with multiple adjacent oval tumour nodules. The latter histologic finding correlated with honeycomb-like signal-poor structures in the OCT image (**b**)

efficiently discriminate between tumour involved and non-involved margins. It reduced the untoward healthy tissue necrosis and provides an encouraging monitoring of the healing process [45]

Melanocytic naevi and malignant melanoma

On OCT images, melanocytic naevi often show an accentuated epidermal layer and elongated rete ridges (Figs. 10, 11). Nests of naevus cells nests are recognized as signal-poor areas with a typical pattern in the apical part of the rete ridges. The more compact the nests of naevus cells are, the better they can be demonstrated [7, 41, 109, 111]. Tumours that are highly pigmented show a stronger scattering of light and have more uniform signal intensity as compared with normal skin. In infiltrative growing melanoma or compound naevi, the second intensity peak which represents the border between the epidermis and dermis may disappear. Again, the penetration depth of melanomas can be measured only in very thin lesions (<1 mm in tumour thickness). Deeper

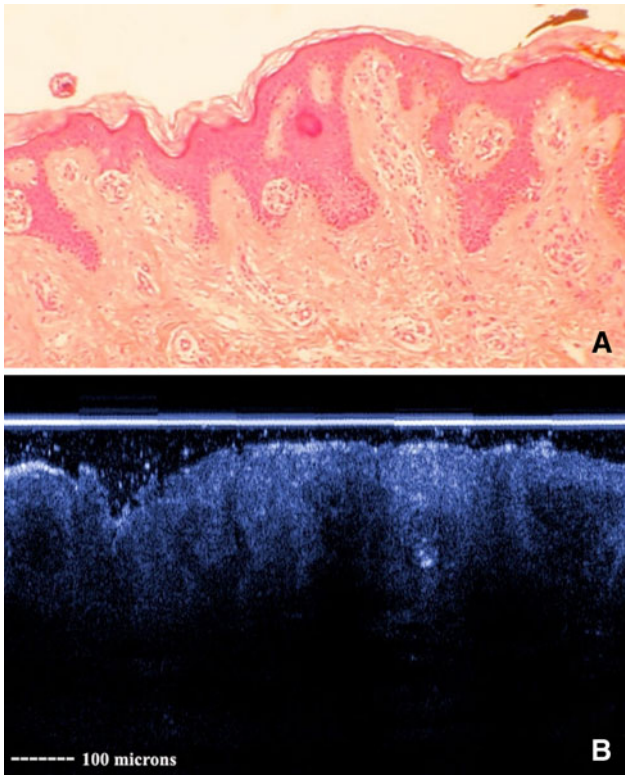

Fig. 10 Histology (haematoxylin–eosin) of a melanocytic naevus (**a**) including the corresponding OCT image (**b**). OCT displays finger-shaped elongated and broadened rete ridges including dense naevus cell clusters. The dermoepidermal junction zone is relatively clearly demarcated from the more or less dark appearing upper dermis (**b**)

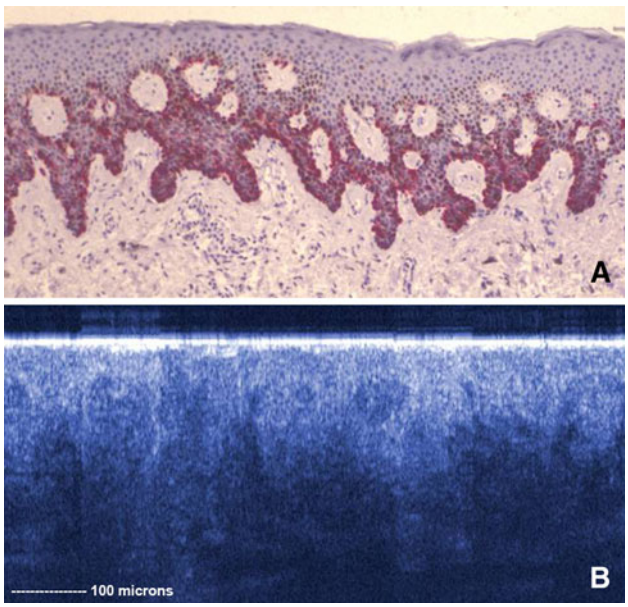

Fig. 11 Immunohistology showing MART-staining of a melanocytic naevus (**a**). On OCT image (**b**), the quite regularly arranged naevus cell nests are visualized

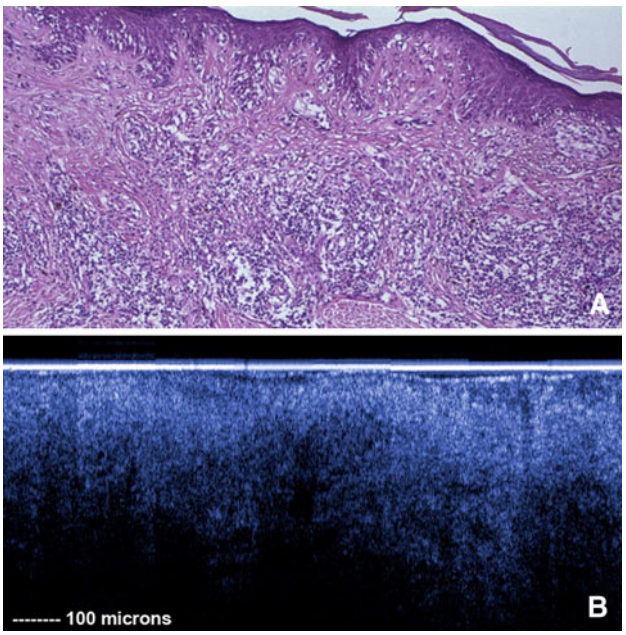

Fig. 12 Histology (**a**, haematoxylin–eosin) a superficial spreading melanoma including the corresponding OCT image (**b**). OCT displays marked architectural disarray including large vertically arranged icicle-shaped structures (**b**)

OCT measurements are barely possible due to the limited penetration depth in skin. We recently performed a systematic trial for the differentiation of benign and malignant melanocytic skin lesions with OCT. We were able to detect significant differences between benign naevi and malignant melanoma in regard to micromorphological features visualized by OCT. In malignant melanoma large vertical, icicle-shaped structures were the most striking OCT feature which did not occur in benign naevi. These distinct OCT features correlated with the histopathological findings (Figs. 12, 13, 14). Therefore, these OCT features might serve as useful discriminating parameters that can be used in future studies investigating the sensitivity and specificity of OCT in melanocytic skin lesions [40]. Previously, another study pointed out that in selected cases OCT allows an in vivo correlation between surface dermoscopic parameters and histopathological correlates, in particular with regard to the pigment network and brown globules. However, the resolution is not high enough to reveal the morphology of single cells, although it is possible to evaluate the architecture of a lesion [16]. Systematic studies for the diagnosis of pigmented lesions with OCT in regard to sensitivity and specificity are still lacking.

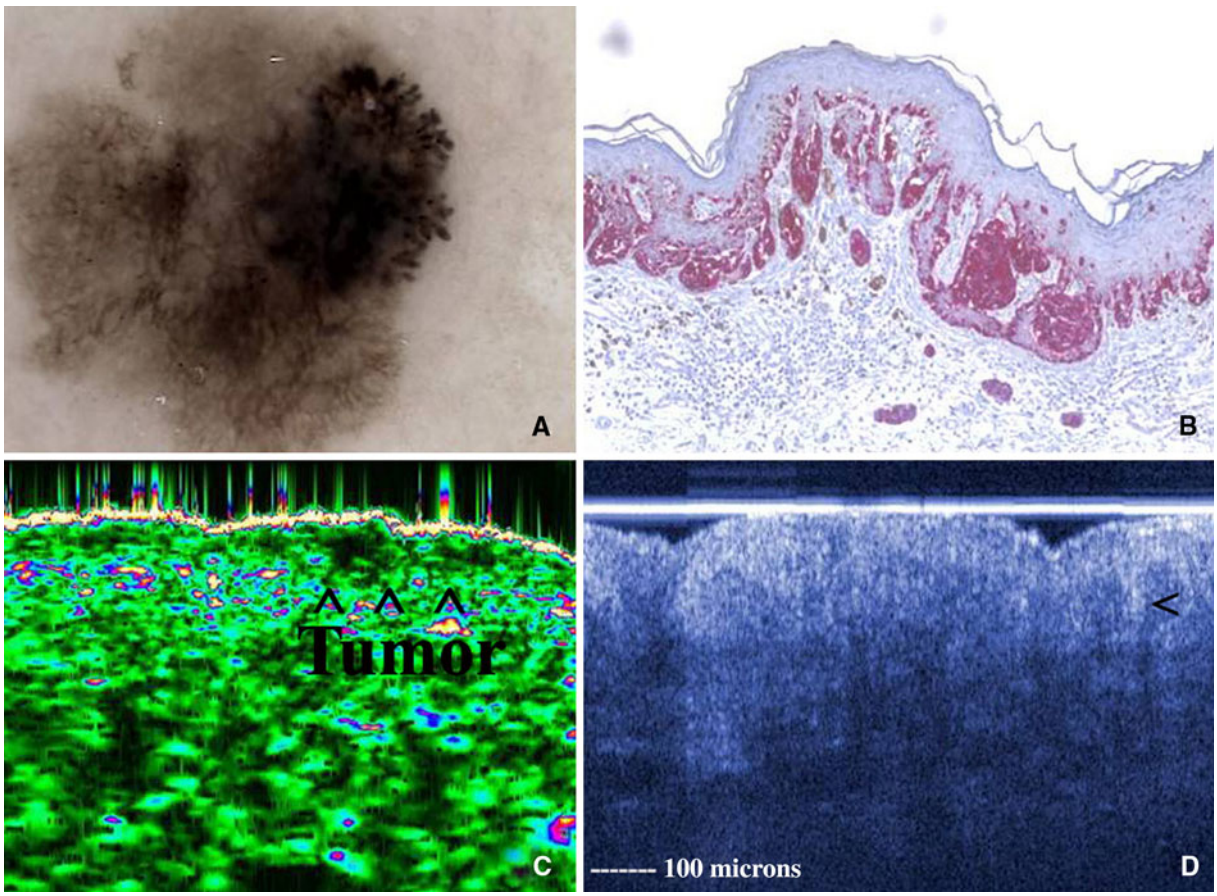

Fig. 13 Showing corresponding images of a superficial spreading melanoma on digital dermoscopy (**a**), immunohistology (MART-staining, **b**), 20 MHz ultrasound (**c**), and OCT displaying elongated rete ridges and tumour cell nests in the upper dermis (**d**)

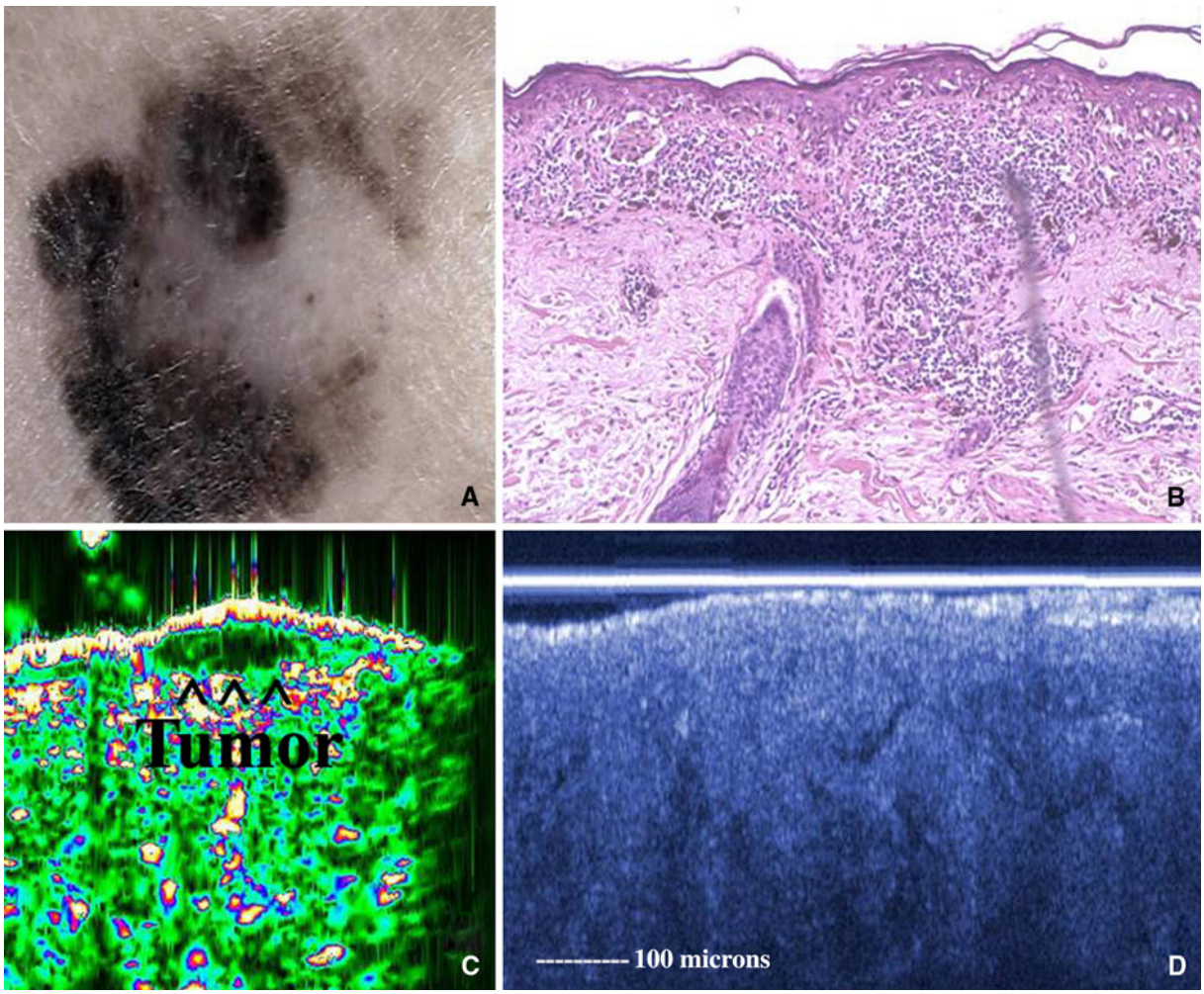

Fig. 14 Superficial spreading melanoma on digital dermoscopy (**a**), histology (**b**), 20 MHz ultrasound (**c**), and OCT showing marked architectural disarray including decreased demarcation of dermoepidermal junction zone and large vertically arranged icicle-shaped structures (**d**)

Evaluation of therapeutic, biophysical and biochemical effects

A variety of therapeutic, biophysical and biochemical effects have been studied in vivo using OCT techniques. These include effects of moisturizers and ointments, glucocorticosteroid-induced skin atrophy, experimentally induced skin inflammation (e.g., dimethyl sulfoxide, nicotinic acid, sodium lauryl sulfate), tape stripping, ultraviolet-induced skin changes and determination of burn as well as freezing depth.

Skin moisture and hydration can be monitored with OCT by determining the refractive index and scattering index, respectively. It was shown that the higher the abundance of water, the lower the refractive index [56, 57]. Our research group was able to confirm these results [87]. Mechanical behaviour of different skin layers and the influence of hydration have also been investigated using OCT in combination with a suction method [46].

Application of various topical agents can transiently change the optical properties of the tissue it is applied on. Treatment of the fingertips with various topical agents (paraffin oil, glycerol, ultrasound gel, 10% urea in petrolatum, petrolatum) induces a decrease of the reflectivity of the skin surface, reflected as a smaller entrance peak in the averaged A-Scan. The lower light attenuation results in an increased penetration depth. The latter effect was shown to be the greatest for paraffin oil among the topical agents studied by Welzel et al. [115]. Experimental animal studies showed that a 50% increase in transmittance and a decrease in diffuse reflectance occur shortly after the application of anhydrous glycerol. The light scattering was also reduced, leading to an increased the depth of visibility with OCT [103, 104].

Skin atrophy induced by the use of a topical glucocorticosteroid was studied by Pagnoni et al. [77]. They were able to objectify a reduction of epidermal thickness from 74 to 61 μm following a 3-week application of 0.05%

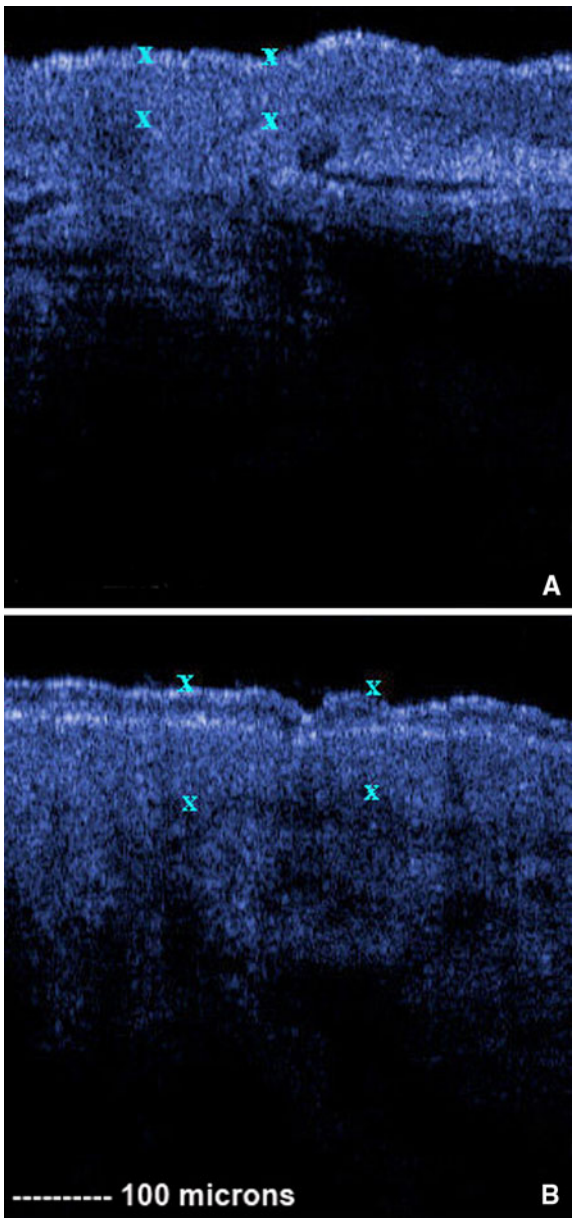

Fig. 15 OCT image at baseline (**a**) and corresponding image 3 days following exposure to three minimal erythema doses of ultraviolet B. A remarkable disruption of the entrance signal with a signal-poor centre is observed (**b**). The *borders* (*x*) between the skin surface and the dermo–epidermal junction are shown indicating an increase of epidermal thickness after ultraviolet B exposure

clobetasol propionate cream. Additionally, they studied the acute effect of dimethyl sulfoxide by means of OCT. A large area of hyporeflection just beneath the superficial signal was seen on OCT images, most likely representing spongiosis of the epidermis. Furthermore, the skin surface became undulating with wider folds. They also observed dilation of signal-free cavities and slight reduction of the light attenuation in the dermis. Comparable changes in OCT images have been seen after the application of histamine and nicotinic acid [115]. The effect of consecutive tape strippings on stratum corneum thickness of glabrous skin could also be quantified using conventional OCT [115].

Various applications of OCT have been tested to monitor burn depth, tissue freezing and wound healing in animal or in vitro models. First, PS-OCT was tested to monitor burn depth after thermal injury. Burn injury denatures the collagen in skin resulting in a reduction of birefringence which can be imaged by PS-OCT through the depth-resolved changes in the polarization state of light radiated and reflected from the skin. This may provide additional information for the physician in order to formulate the optimal treatment [96]. Additionally, high-speed optical coherence and Doppler tomography systems were tested for real-time monitoring of the microstructural and microvascular tissue changes induced by laser thermal therapy [119]. Accordingly, OCT was used for monitoring the wound healing after laser thermal injury [120].

OCT has also been successfully used for the monitoring of skin equivalents and tissue-engineered skin at different stages of the culture process [93, 94]. Furthermore, Choi et al. [11] have demonstrated that OCT may be used as a feedback tool during cryosurgical procedures to monitor progression of the freezing front.

Our study group intensely investigated the ultraviolet (UV)-induced skin changes by means of OCT [31, 32, 34]. UV-induced skin changes such as parakeratosis and epidermal thickening can be identified and quantified by means of OCT (Fig. 15). Alterations of the scattering coefficient of different skin layers following UVA-induced pigmentation has also been described [31, 34, 115]. A comparison of OCT versus confocal laser scanning microscopy for evaluating in vivo dose and time-dependent skin changes following solar-simulated irradiation, could not demonstrate superiority of one technique over the other [32]. In conclusion, OCT may be a promising tool for photobiological studies aimed at assessing and monitoring photoadaptive and phototoxic processes in vivo [31, 32, 34, 66].

Competing in vivo skin imaging techniques

The clinical application of ultrasound transducer technology (20-MHz) in dermatology includes the evaluation of tissue oedema, wound healing and imaging of skin and tumour thickness. The investigation of tumour thickness is of particular interest in patients with malignant melanoma (Figs. 13, 14). Encouraging results have been obtained with ultrasound transducers in the range of 40–50 MHz (lateral resolution about 50 μm) and technical modifications including ultrasound backscatter microscopy. In order to investigate the epidermis, however, both the lateral and

axial resolutions of current devices need to be improved. Ultrasound transducers with centre frequencies of about 100 MHz are expected to be used for future diagnostic tissue characterization because of their high lateral resolution of about 10–20 μm [36, 60]. Confocal scanning laser microscopy is an in vivo and non-invasive technology that examines the skin at a resolution comparable to that of histology [4, 5, 32, 78, 88]. When compared with the OCT and high-frequency ultrasound, confocal laser scanning microscopy offers the highest resolution imaging (lateral resolution of about 1 μm; penetration depth 300–400 μm) comparable to routine histology [39]. Unlike ultrasound, OCT and routine histology, confocal microscopy visualizes skin structures on a horizontal plane. With regard to lateral resolution, ultra-high resolution OCT, confocal microscopy and multiphoton laser microscopy are indisputably superior to ultrasound scanners and conventional OCT as well. Nevertheless, these methods are limited in depth penetration [120].

Comment and outlook

OCT is a useful non-invasive technology for the diagnosis and monitoring of a variety of skin conditions. Using conventional OCT various micro-morphological and architectural features of healthy skin can be studied such as the stratum corneum (palmoplantar), the epidermis, and upper dermis, as well as skin appendages and blood vessels. Moreover, pathological changes have been identified and visualized in many conditions including inflammatory skin diseases and benign and malignant cutaneous neoplasms. Since OCT imaging is non-traumatic, reproducible and well-tolerated, it is also well suitable for disease monitoring and evaluation of treatment effects over time. Functional OCT imaging based on spectroscopy, tissue birefringence and Doppler flow, represents already a real progress for dermatological purposes as well. OCT has active research community with a high number of publications, demonstrating the immense potential of this imaging method. The most promising technological development in OCT is the combination of standard OCT and techniques that analyse more optical properties compared with pure backscattering. State-of-the-art OCT systems already implement Doppler techniques to measure the flow velocity of blood. Also polarization-sensitive devices are available for the research community. The combination of OCT and spectroscopy has been demonstrated by several groups around the world, but some technical problems have not been solved yet. Since spectroscopic methods are part of diagnostics by now, a combination with the depth information in OCT seems to be a highly interesting field. It has, however, to be stressed that most previous studies of OCT in the field of dermatology and closely related specialities had an exploratory character and were frequently performed only on very small study samples. Hence, more comprehensive biomedical and systematic clinical studies are required to develop and validate the applications of OCT in dermatology. These studies will be challenging because of stringent statistical performance criteria, such as sensitivity and specificity and must be evaluated on an application-by-application basis. It is unlikely that OCT will completely replace conventional skin biopsy and histology or other existing diagnostic modalities. However, from the point of view of non-invasive diagnosis of skin diseases and monitoring of treatment effects over time, in particular, the aforementioned advanced versions of OCT might lead in near future to significant new insights into skin physiology, pathology and therapeutic control of skin disorders. Combination of OCT with other imaging techniques—so called multi-modality imaging such as Raman, Doppler, fluorescence and ultrasound—may further improve diagnostic capabilities in skin research as well as future dermatology practice.

References

1. Aalders MC, Triesscheijn M, Ruevekamp M, de Bruin M, Baas P, Faber DJ, Stewart FA (2006) Doppler optical coherence tomography to monitor the effect of photodynamic therapy on tissue morphology and perfusion. J Biomed Opt 11(4):044011. doi:10.1117/1.2337302
2. Abuzahra F, Spoler F, Forst M, Brans R, Erdmann S, Merk HF, Obrigkeit DH (2010) Pilot study: optical coherence tomography as a non-invasive diagnostic perspective for real time visualisation of onychomycosis. Mycoses 53(4):334–339. doi:10.1111/j.1439-0507.2009.01717.x
3. Alex A, Povazay B, Hofer B, Popov S, Glittenberg C, Binder S, Drexler W (2010) Multispectral in vivo three-dimensional optical coherence tomography of human skin. J Biomed Opt 15(2):026025. doi:10.1117/1.3400665
4. Altintas MA, Altintas AA, Guggenheim M, Niederbichler AD, Knobloch K, Vogt PM (2009) In vivo evaluation of histomorphological alterations in first-degree burn injuries by means of confocal-laser-scanning microscopy-more than "virtual histology?". J Burn Care Res 30(2):315–320. doi:10.1097/BCR.0b013e318198e746
5. Altintas MA, Altintas AA, Guggenheim M, Steiert AE, Aust MC, Niederbichler AD, Herold C, Vogt PM (2010) Insight in human skin microcirculation using in vivo reflectance-mode confocal laser scanning microscopy. J Digit Imaging 23(4):475–481. doi:10.1007/s10278-009-9219-3
6. Barton JK, Gossage KW, Xu W, Ranger-Moore JR, Saboda K, Brooks CA, Duckett LD, Salasche SJ, Warneke JA, Alberts DS (2003) Investigating sun-damaged skin and actinic keratosis with optical coherence tomography: a pilot study. Technol Cancer Res Treat 2(6):525–535
7. Bechara FG, Gambichler T, Stucker M, Orlikov A, Rotterdam S, Altmeyer P, Hoffmann K (2004) Histomorphologic correlation with routine histology and optical coherence tomography. Skin

Res Technol 10(3):169–173. doi:10.1111/j.1600-0846.2004.00038.x
8. Buder K, Knuschke P, Wozel G (2010) Evaluation of methylprednisolone aceponate, tacrolimus and combination thereof in the psoriasis plaque test using sum score, 20-MHz-ultrasonography and optical coherence tomography. Int J Clin Pharmacol Ther 48(12):814–820
9. Cahill RA, Mortensen NJ (2010) Intraoperative augmented reality for laparoscopic colorectal surgery by intraoperative near-infrared fluorescence imaging and optical coherence tomography. Minerva Chir 65(4):451–462
10. Chen Z, Milner TE, Srinivas S, Wang X, Malekafzali A, van Gemert MJ, Nelson JS (1997) Noninvasive imaging of in vivo blood flow velocity using optical Doppler tomography. Opt Lett 22(14):1119–1121
11. Choi B, Milner TE, Kim J, Goodman JN, Vargas G, Aguilar G, Nelson JS (2004) Use of optical coherence tomography to monitor biological tissue freezing during cryosurgery. J Biomed Opt 9(2):282–286. doi:10.1117/1.1648647
12. Choma M, Sarunic M, Yang C, Izatt J (2003) Sensitivity advantage of swept source and Fourier domain optical coherence tomography. Opt Express 11(18):2183–2189
13. Chu CR, Izzo NJ, Irrgang JJ, Ferretti M, Studer RK (2007) Clinical diagnosis of potentially treatable early articular cartilage degeneration using optical coherence tomography. J Biomed Opt 12(5):051703. doi:10.1117/1.2789674
14. Cimalla P, Walther J, Mehner M, Cuevas M, Koch E (2009) Simultaneous dual-band optical coherence tomography in the spectral domain for high resolution in vivo imaging. Opt Express 17(22):19486–19500. doi:10.1364/OE.17.019486
15. de Boer JF, Cense B, Park BH, Pierce MC, Tearney GJ, Bouma BE (2003) Improved signal-to-noise ratio in spectral-domain compared with time-domain optical coherence tomography. Opt Lett 28(21):2067–2069
16. de Giorgi V, Stante M, Massi D, Mavilia L, Cappugi P, Carli P (2005) Possible histopathologic correlates of dermoscopic features in pigmented melanocytic lesions identified by means of optical coherence tomography. Exp Dermatol 14(1):56–59. doi:10.1111/j.0906-6705.2005.00229.x
17. Drexler W (2004) Ultrahigh-resolution optical coherence tomography. J Biomed Opt 9(1):47–74. doi:10.1117/1.1629679
18. Drexler W, Andersen PE (2009) Optical coherence tomography in biophotonics. J Biophotonics 2(6–7):339–341. doi:10.1002/jbio.200910542
19. Faber DJ, Mik EG, Aalders MC, van Leeuwen TG (2005) Toward assessment of blood oxygen saturation by spectroscopic optical coherence tomography. Opt Lett 30(9):1015–1017
20. Fan C, Wang Y, Wang RK (2007) Spectral domain polarization sensitive optical coherence tomography achieved by single camera detection. Opt Express 15(13):7950–7961
21. Fercher AF (1993) Ophthalmic interferometry. In: von Bally G, Khanna S (eds) Optics in medicine, biology and environmental research. Selected contributions to the First International Conference on Optics Within Life Sciences (OLWS I), Garmisch-Partenkirchen, Germany, 12–16 August 1990 (ICO-15 SAT). Elsevier, Amsterdam, pp 221–228
22. Fercher AF (2008) Inverse scattering, dispersion and speckle in optical coherence tomography. In: Drexler W, Fujimoto JG (eds) Optical coherence tomography, pp 119–146
23. Fercher AF, Roth E (1986) Ophthalmic laser interferometry. In: Proceedings of the SPIE—The International Society for Optical Engineering, vol 658, pp 48–51
24. Fercher AF, Hitzenberger CK, Drexler W, Kamp G, Sattmann H (1993) In vivo optical coherence tomography. Am J Ophthalmol 116(1):113–114
25. Fercher AF, Mengedoht K, Werner W (1988) Eye-length measurement by interferometry with partially coherent light. Opt Lett 13(3):186–188
26. Forsea AM, Carstea EM, Ghervase L, Giurcaneanu C, Pavelescu G (2010) Clinical application of optical coherence tomography for the imaging of non-melanocytic cutaneous tumors: a pilot multi-modal study. J Med Life 3(4):381–389
27. Fruhstorfer H, Abel U, Garthe CD, Knuttel A (2000) Thickness of the stratum corneum of the volar fingertips. Clin Anat 13(6):429–433. doi:10.1002/1098-2353(2000)13:6<429
28. Fujimoto JG (2003) Optical coherence tomography for ultrahigh resolution in vivo imaging. Nat Biotechnol 21(11):1361–1367. doi:10.1038/nbt892
29. Gambichler T, Boms S, Stucker M, Kreuter A, Moussa G, Sand M, Altmeyer P, Hoffmann K (2006) Epidermal thickness assessed by optical coherence tomography and routine histology: preliminary results of method comparison. J Eur Acad Dermatol Venereol 20(7):791–795. doi:10.1111/j.1468-3083.2006.01629.x
30. Gambichler T, Boms S, Stucker M, Kreuter A, Sand M, Moussa G, Altmeyer P, Hoffmann K (2005) Comparison of histometric data obtained by optical coherence tomography and routine histology. J Biomed Opt 10(4):44008. doi:10.1117/1.2039086
31. Gambichler T, Boms S, Stucker M, Moussa G, Kreuter A, Sand M, Sand D, Altmeyer P, Hoffmann K (2005) Acute skin alterations following ultraviolet radiation investigated by optical coherence tomography and histology. Arch Dermatol Res 297(5):218–225. doi:10.1007/s00403-005-0604-6
32. Gambichler T, Huyn J, Tomi NS, Moussa G, Moll C, Sommer A, Altmeyer P, Hoffmann K (2006) A comparative pilot study on ultraviolet-induced skin changes assessed by noninvasive imaging techniques in vivo. Photochem Photobiol 82(4):1103–1107. doi:10.1562/2005-12-21-RA-757
33. Gambichler T, Hyun J, Moussa G, Tomi NS, Boms S, Altmeyer P, Hoffmann K, Kreuter A (2007) Optical coherence tomography of cutaneous lupus erythematosus correlates with histopathology. Lupus 16(1):35–38
34. Gambichler T, Kunzlberger B, Paech V, Kreuter A, Boms S, Bader A, Moussa G, Sand M, Altmeyer P, Hoffmann K (2005) UVA1 and UVB irradiated skin investigated by optical coherence tomography in vivo: a preliminary study. Clin Exp Dermatol 30(1):79–82. doi:10.1111/j.1365-2230.2004.01690.x
35. Gambichler T, Matip R, Moussa G, Altmeyer P, Hoffmann K (2006) In vivo data of epidermal thickness evaluated by optical coherence tomography: effects of age, gender, skin type, and anatomic site. J Dermatol Sci 44(3):145–152. doi:10.1016/j.jdermsci.2006.09.008
36. Gambichler T, Moussa G, Bahrenberg K, Vogt M, Ermert H, Weyhe D, Altmeyer P, Hoffmann K (2007) Preoperative ultrasonic assessment of thin melanocytic skin lesions using a 100-MHz ultrasound transducer: a comparative study. Dermatol Surg 33(7):818–824. doi:10.1111/j.1524-4725.2007.33175.x
37. Gambichler T, Moussa G, Regeniter P, Kasseck C, Hofmann MR, Bechara FG, Sand M, Altmeyer P, Hoffmann K (2007) Validation of optical coherence tomography in vivo using cryostat histology. Phys Med Biol 52(5):N75–N85. doi:10.1088/0031-9155/52/5/N01
38. Gambichler T, Moussa G, Sand M, Sand D, Orlikov A, Altmeyer P, Hoffmann K (2005) Correlation between clinical scoring of allergic patch test reactions and optical coherence tomography. J Biomed Opt 10(6):064030. doi:10.1117/1.2141933
39. Gambichler T, Orlikov A, Vasa R, Moussa G, Hoffmann K, Stucker M, Altmeyer P, Bechara FG (2007) In vivo optical coherence tomography of basal cell carcinoma. J Dermatol Sci 45(3):167–173. doi:10.1016/j.jdermsci.2006.11.012

40. Gambichler T, Regeniter P, Bechara FG, Orlikov A, Vasa R, Moussa G, Stucker M, Altmeyer P, Hoffmann K (2007) Characterization of benign and malignant melanocytic skin lesions using optical coherence tomography in vivo. J Am Acad Dermatol 57(4):629–637. doi:10.1016/j.jaad.2007.05.029
41. Gladkova ND, Petrova GA, Nikulin NK, Radenska-Lopovok SG, Snopova LB, Chumakov YP, Nasonova VA, Gelikonov VM, Gelikonov GV, Kuranov RV, Sergeev AM, Feldchtein FI (2000) In vivo optical coherence tomography imaging of human skin: norm and pathology. Skin Res Technol 6(1):6–16
42. Glogau RG (2000) The risk of progression to invasive disease. J Am Acad Dermatol 42(1):23–24
43. Gotzinger E, Pircher M, Geitzenauer W, Ahlers C, Baumann B, Michels S, Schmidt-Erfurth U, Hitzenberger CK (2008) Retinal pigment epithelium segmentation by polarization sensitive optical coherence tomography. Opt Express 16(21):16410–16422
44. Graf RN, Robles F, Chen X, Wax A (2010) Detecting precancerous lesions in the hamster cheek pouch using spectroscopic white-light optical coherence tomography to assess nuclear morphology via spectral oscillations. J Biomed Opt 14(6):064030. doi:10.1117/1.3269680
45. Hamdoon Z, Jerjes W, Upile T, Hopper C (2011) Optical coherence tomography-guided photodynamic therapy for skin cancer: case study. Photodiagnosis Photodyn Ther 8(1):49–52. doi:10.1016/j.pdpdt.2010.08.004
46. Hendriks FM, Brokken D, Oomens CW, Baaijens FP (2004) Influence of hydration and experimental length scale on the mechanical response of human skin in vivo, using optical coherence tomography. Skin Res Technol 10(4):231–241. doi:10.1111/j.1600-0846.2004.00077.x
47. Holmes J, Hattersley S (2009) Image blending and speckle noise reduction in multi-beam OCT. Proc SPIE 7168(1):71681N. doi:10.1117/12.808575
48. Huang D, Swanson EA, Lin CP, Schuman JS, Stinson WG, Chang W, Hee MR, Flotte T, Gregory K, Puliafito CA, Fujimoto JG et al (1991) Optical coherence tomography. Science 254(5035):1178–1181
49. Izatt JA, Kulkarni MD, Yazdanfar S, Barton JK, Welch AJ (1997) In vivo bidirectional color Doppler flow imaging of picoliter blood volumes using optical coherence tomography. Opt Lett 22(18):1439–1441
50. Jorgensen TM, Tycho A, Mogensen M, Bjerring P, Jemec GB (2008) Machine-learning classification of non-melanoma skin cancers from image features obtained by optical coherence tomography. Skin Res Technol 14(3):364–369. doi:10.1111/j.1600-0846.2008.00304.x
51. Josse G, George J, Black D (2011) Automatic measurement of epidermal thickness from optical coherence tomography images using a new algorithm. Skin Res Technol. doi:10.1111/j.1600-0846.2011.00499.x
52. Kartakoullis A, Bousi E, Pitris C (2010) Scatterer size-based analysis of optical coherence tomography images using spectral estimation techniques. Opt Express 18(9):9181–9191. doi:10.1364/OE.18.009181
53. Kasseck C, Jaedicke V, Gerhardt NC, Welp H, Hofmann MR (2010) Substance identification by depth resolved spectroscopic pattern reconstruction in frequency domain optical coherence tomography. Opt Commun 283(23):4816–4822
54. Kennedy BF, Hillman TR, McLaughlin RA, Quirk BC, Sampson DD (2009) In vivo dynamic optical coherence elastography using a ring actuator. Opt Express 17(24):21762–21772. doi:10.1364/OE.17.021762
55. Khandwala M, Penmetsa BR, Dey S, Schofield JB, Jones CA (2010) Podoleanu a imaging of periocular basal cell carcinoma using en face optical coherence tomography: a pilot study. Br J Ophthalmol 94(10):1332–1336. doi:10.1136/bjo.2009.170811
56. Knuttel A, Boehlau-Godau M (2000) Spatially confined and temporally resolved refractive index and scattering evaluation in human skin performed with optical coherence tomography. J Biomed Opt 5(1):83–92. doi:10.1117/1.429972
57. Knuttel A, Bonev S, Knaak W (2004) New method for evaluation of in vivo scattering and refractive index properties obtained with optical coherence tomography. J Biomed Opt 9(2):265–273. doi:10.1117/1.1647544
58. Kodach VM, Faber DJ, van Marle J, van Leeuwen TG, Kalkman J (2011) Determination of the scattering anisotropy with optical coherence tomography. Opt Express 19(7):6131–6140
59. Konig K, Speicher M, Buckle R, Reckfort J, McKenzie G, Welzel J, Koehler MJ, Elsner P, Kaatz M (2009) Clinical optical coherence tomography combined with multiphoton tomography of patients with skin diseases. J Biophotonics 2(6–7):389–397. doi:10.1002/jbio.200910013
60. Korde VR, Bonnema GT, Xu W, Krishnamurthy C, Ranger-Moore J, Saboda K, Slayton LD, Salasche SJ, Warneke JA, Alberts DS, Barton JK (2007) Using optical coherence tomography to evaluate skin sun damage and precancer. Lasers Surg Med 39(9):687–695. doi:10.1002/lsm.20573
61. Lamirel C, Newman N, Biousse V (2009) The use of optical coherence tomography in neurology. Rev Neurol Dis 6(4):E105–E120
62. Lankenau E, Welzel J, Birngruber R, Engelhardt R (1997) In Vivo Tissue Measurements with Optical low Coherence Tomography. In: Tuchin V, Podbielska H, Ovrin B (eds) Coherence domain optical methods in biomedical science and clinical applications. Proc Soc Photo-Opt Instrum Eng, SPIE. 2981:78–84
63. Leitgeb R, Hitzenberger C, Fercher A (2003) Performance of fourier domain vs time domain optical coherence tomography. Opt Express 11(8):889–894
64. Leitgeb R, Schmetterer L, Drexler W, Fercher A, Zawadzki R, Bajraszewski T (2003) Real-time assessment of retinal blood flow with ultrafast acquisition by color Doppler Fourier domain optical coherence tomography. Opt Express 11(23):3116–3121
65. Leitgeb R, Wojtkowski M, Kowalczyk A, Hitzenberger CK, Sticker M, Fercher AF (2000) Spectral measurement of absorption by spectroscopic frequency-domain optical coherence tomography. Opt Lett 25(11):820–822
66. Liu Z, Guo Z, Zhuang Z, Zhai J, Xiong H, Zeng C (2010) Quantitative optical coherence tomography of skin lesions induced by different ultraviolet B sources. Phys Med Biol 55(20):6175–6185. doi:10.1088/0031-9155/55/20/009
67. Mogensen M, Joergensen TM, Nurnberg BM, Morsy HA, Thomsen JB, Thrane L, Jemec GB (2009) Assessment of optical coherence tomography imaging in the diagnosis of non-melanoma skin cancer and benign lesions versus normal skin: observer-blinded evaluation by dermatologists and pathologists. Dermatol Surg 35(6):965–972. doi:10.1111/j.1524-4725.2009.01164.x
68. Mogensen M, Morsy HA, Nurnberg BM, Jemec GB (2008) Optical coherence tomography imaging of bullous diseases. J Eur Acad Dermatol Venereol 22(12):1458–1464. doi:10.1111/j.1468-3083.2008.02917.x
69. Mogensen M, Morsy HA, Thrane L, Jemec GB (2008) Morphology and epidermal thickness of normal skin imaged by optical coherence tomography. Dermatology 217(1):14–20. doi:10.1159/000118508
70. Mogensen M, Nurnberg BM, Forman JL, Thomsen JB, Thrane L, Jemec GB (2009) In vivo thickness measurement of basal cell carcinoma and actinic keratosis with optical coherence

tomography and 20-MHz ultrasound. Br J Dermatol 160(5):1026–1033. doi:10.1111/j.1365-2133.2008.09003.x
71. Mogensen M, Thrane L, Jorgensen TM, Andersen PE, Jemec GB (2009) OCT imaging of skin cancer and other dermatological diseases. J Biophotonics 2(6–7):442–451. doi:10.1002/jbio.200910020
72. Morgner U, Drexler W, Kartner FX, Li XD, Pitris C, Ippen EP, Fujimoto JG (2000) Spectroscopic optical coherence tomography. Opt Lett 25(2):111–113
73. Morsy H, Kamp S, Thrane L, Behrendt N, Saunder B, Zayan H, Elmagid EA, Jemec GB (2010) Optical coherence tomography imaging of psoriasis vulgaris: correlation with histology and disease severity. Arch Dermatol Res 302(2):105–111. doi:10.1007/s00403-009-1000-4
74. Neerken S, Lucassen GW, Bisschop MA, Lenderink E, Nuijs TA (2004) Characterization of age-related effects in human skin: a comparative study that applies confocal laser scanning microscopy and optical coherence tomography. J Biomed Opt 9(2):274–281. doi:10.1117/1.1645795
75. Nelson JS, Kelly KM, Zhao Y, Chen Z (2001) Imaging blood flow in human port-wine stain in situ and in real time using optical Doppler tomography. Arch Dermatol 137(6):741–744
76. Olmedo JM, Warschaw KE, Schmitt JM, Swanson DL (2006) Optical coherence tomography for the characterization of basal cell carcinoma in vivo: a pilot study. J Am Acad Dermatol 55(3):408–412. doi:10.1016/j.jaad.2006.03.013
77. Pagnoni A, Knüttel A, Welker P, Rist M, Stoudemayer T, Kolbe L, Sadiq I, Kligman A (1999) Optical coherence tomography in dermatology. Skin Res Technol 5:83–87
78. Patel JK, Konda S, Perez OA, Amini S, Elgart G, Berman B (2008) Newer technologies/techniques and tools in the diagnosis of melanoma. Eur J Dermatol 18(6):617–631. doi:10.1684/ejd.2008.0508
79. Pierce MC, Strasswimmer J, Hyle Park B, Cense B, De Boer JF (2004) Birefringence measurements in human skin using polarization-sensitive optical coherence tomography. J Biomed Opt 9(2):287–291. doi:10.1117/1.1645797
80. Pircher M, Gotzinger E, Leitgeb R, Fercher A, Hitzenberger C (2003) Measurement and imaging of water concentration in human cornea with differential absorption optical coherence tomography. Opt Express 11(18):2190–2197
81. Robles F, Graf RN, Wax A (2009) Dual window method for processing spectroscopic optical coherence tomography signals with simultaneously high spectral and temporal resolution. Opt Express 17(8):6799–6812
82. Robles FE, Chowdhury S, Wax A (2010) Assessing hemoglobin concentration using spectroscopic optical coherence tomography for feasibility of tissue diagnostics. Opt Express 1(1):310–317
83. Sacchet D, Moreau J, Georges P, Dubois A (2008) Simultaneous dual-band ultra-high resolution full-field optical coherence tomography. Opt Express 16(24):19434–19446
84. Sainter AW, King TA, Dickinson MR (2004) Effect of target biological tissue and choice of light source on penetration depth and resolution in optical coherence tomography. J Biomed Opt 9(1):193–199. doi:10.1117/1.1628243
85. Sakai S, Nakagawa N, Yamanari M, Miyazawa A, Yasuno Y, Matsumoto M (2009) Relationship between dermal birefringence and the skin surface roughness of photoaged human skin. J Biomed Opt 14(4):044032. doi:10.1117/1.3207142
86. Salvini C, Massi D, Cappetti A, Stante M, Cappugi P, Fabbri P, Carli P (2008) Application of optical coherence tomography in non-invasive characterization of skin vascular lesions. Skin Res Technol 14(1):89–92. doi:10.1111/j.1600-0846.2007.00265.x
87. Sand M, Gambichler T, Moussa G, Bechara FG, Sand D, Altmeyer P, Hoffmann K (2006) Evaluation of the epidermal refractive index measured by optical coherence tomography. Skin Res Technol 12(2):114–118. doi:10.1111/j.0909-752X.2006.00144.x
88. Sauermann K, Gambichler T, Wilmert M, Rotterdam S, Stucker M, Altmeyer P, Hoffmann K (2002) Investigation of basal cell carcinoma [correction of carcionoma] by confocal laser scanning microscopy in vivo. Skin Res Technol 8(3):141–147
89. Saxer CE, de Boer JF, Park BH, Zhao Y, Chen Z, Nelson JS (2000) High-speed fiber based polarization-sensitive optical coherence tomography of in vivo human skin. Opt Lett 25(18):1355–1357
90. Schmitt J (1998) OCT elastography: imaging microscopic deformation and strain of tissue. Opt Express 3(6):199–211
91. Schmitt JM (1999) Optical coherence tomography. IEEE J Sel Top Quantum Electr 5:1205–1215
92. Schmitt JM (1999) Optical coherence tomography (OCT): a review. IEEE J Sel Top Quantum Electr 5(4):1205–1215
93. Smith LE, Bonesi M, Smallwood R, Matcher SJ, Macneil S (2010) Using swept-source optical coherence tomography to monitor the formation of neo-epidermis in tissue-engineered skin. J Tissue Eng Regen Med. doi:10.1002/term.281
94. Spoler F, Forst M, Marquardt Y, Hoeller D, Kurz H, Merk H, Abuzahra F (2006) High-resolution optical coherence tomography as a non-destructive monitoring tool for the engineering of skin equivalents. Skin Res Technol 12(4):261–267. doi:10.1111/j.0909-752X.2006.00163.x
95. Spoler F, Kray S, Grychtol P, Hermes B, Bornemann J, Forst M, Kurz H (2007) Simultaneous dual-band ultra-high resolution optical coherence tomography. Opt Express 15(17):10832–10841
96. Srinivas SM, de Boer JF, Park H, Keikhanzadeh K, Huang HE, Zhang J, Jung WQ, Chen Z, Nelson JS (2004) Determination of burn depth by polarization-sensitive optical coherence tomography. J Biomed Opt 9(1):207–212. doi:10.1117/1.1629680
97. Strasswimmer J, Pierce MC, Park BH, Neel V, de Boer JF (2004) Polarization-sensitive optical coherence tomography of invasive basal cell carcinoma. J Biomed Opt 9(2):292–298. doi:10.1117/1.1644118
98. Tang S, Krasieva TB, Chen Z, Tempea G, Tromberg BJ (2006) Effect of pulse duration on two-photon excited fluorescence and second harmonic generation in nonlinear optical microscopy. J Biomed Opt 11(2):020501. doi:10.1117/1.2177676
99. Tearney GJ, Brezinski ME, Bouma BE, Boppart SA, Pitris C, Southern JF, Fujimoto JG (1997) In vivo endoscopic optical biopsy with optical coherence tomography. Science 276(5321):2037–2039
100. Thomas MW, Grichnik JM, Izatt JA (2007) Three-dimensional images and vessel rendering using optical coherence tomography. Arch Dermatol 143(11):1468–1469. doi:10.1001/archderm.143.11.1468
101. Unterhuber A, Povazay B, Bizheva K, Hermann B, Sattmann H, Stingl A, Le T, Seefeld M, Menzel R, Preusser M, Budka H, Schubert C, Reitsamer H, Ahnelt PK, Morgan JE, Cowey A, Drexler W (2004) Advances in broad bandwidth light sources for ultrahigh resolution optical coherence tomography. Phys Med Biol 49(7):1235–1246
102. Vakoc B, Yun S, de Boer J, Tearney G, Bouma B (2005) Phase-resolved optical frequency domain imaging. Opt Express 13(14):5483–5493
103. Vargas G, Chan EK, Barton JK, Rylander HG 3rd, Welch AJ (1999) Use of an agent to reduce scattering in skin. Lasers Surg Med 24(2):133–141. doi:10.1002/(SICI)1096-9101
104. Vargas G, Readinger A, Dozier SS, Welch AJ (2003) Morphological changes in blood vessels produced by hyperosmotic agents and measured by optical coherence tomography. Photochem Photobiol 77(5):541–549
105. Vo-Dinh T (ed) (2003) Biomedical Photonics Handbook, 1 edn. SPIE, CRC Press, Boca Raton

106. Wang L, Wang Y, Guo S, Zhang J, Bachman M (2004) Frequency domain phase-resolved optical Doppler and Doppler variance tomography optics communications 242(4–6):345–350
107. Wang Y, Zhao Y, Nelson JS, Chen Z, Windeler RS (2003) Ultrahigh-resolution optical coherence tomography by broadband continuum generation from a photonic crystal fiber. Opt Lett 28(3):182–184
108. Weissman J, Hancewicz T, Kaplan P (2004) Optical coherence tomography of skin for measurement of epidermal thickness by shapelet-based image analysis. Opt Express 12(23):5760–5769
109. Welzel J (2001) Optical coherence tomography in dermatology: a review. Skin Res Technol 7(1):1–9
110. Welzel J, Bruhns M, Wolff HH (2003) Optical coherence tomography in contact dermatitis and psoriasis. Arch Dermatol Res 295(2):50–55. doi:10.1007/s00403-003-0390-y
111. Welzel J, Lankenau E, Birngruber R, Engelhardt R (1997) Optical coherence tomography of the human skin. J Am Acad Dermatol 37(6):958–963, S0190-9622(97)70072-0 [pii]
112. Welzel J, Lankenau E, Birngruber R, Engelhardt R (1998) Optical coherence tomography of the skin. Curr Probl Dermatol 26:27–37
113. Welzel J, Lankenau E, Hüttmann G, Birngruber R (eds) (2008) OCT in dermatology. Handbook of optical coherence tomography. Springer, Berlin
114. Welzel J, Noack J, Lankenau E, Engelhardt R (2002) Optical coherence tomography in dermatology. Handbook of optical coherence tomography. Marcel Dekker, Inc., New York
115. Welzel J, Reinhardt C, Lankenau E, Winter C, Wolff HH (2004) Changes in function and morphology of normal human skin: evaluation using optical coherence tomography. Br J Dermatol 150(2):220–225
116. Wieser W, Biedermann BR, Klein T, Eigenwillig CM, Huber R (2010) Multi-megahertz OCT: high quality 3D imaging at 20 million A-scans and 4.5 GVoxels per second. Opt Express 18(14):14685–14704. doi:10.1364/OE.18.014685
117. Wilder-Smith P, Krasieva T, Jung WG, Zhang J, Chen Z, Osann K, Tromberg B (2005) Noninvasive imaging of oral premalignancy and malignancy. J Biomed Opt 10(5):051601. doi:10.1117/1.2098930
118. Xu C, Kamalabadi F, Boppart SA (2005) Comparative performance analysis of time-frequency distributions for spectroscopic optical coherence tomography. Appl Opt 44(10):1813–1822
119. Yang VXD, Pekar J, Lo SSW, Gordon ML, Wilson BC, Vitkina IA (2003) Optical coherence and Doppler tomography for monitoring tissue changes induced by laser thermal therapy—An in vivo feasibility study. Rev Sci Instrum 74(1):437–440
120. Yeh AT, Kao B, Jung WG, Chen Z, Nelson JS, Tromberg BJ (2004) Imaging wound healing using optical coherence tomography and multiphoton microscopy in an in vitro skin-equivalent tissue model. J Biomed Opt 9(2):248–253. doi:10.1117/1.1648646
121. Zhang J, Chen Z (2005) In vivo blood flow imaging by a swept laser source based Fourier domain optical Doppler tomography. Opt Express 13(19):7449–7457
122. Zhao S, Gu Y, Xue P, Guo J, Shen T, Wang T, Huang N, Zhang L, Qiu H, Yu X, Wei X (2010) Imaging port wine stains by fiber optical coherence tomography. J Biomed Opt 15(3):036020. doi:10.1117/1.3445712
123. Zhao Y, Chen Z, Saxer C, Xiang S, de Boer JF, Nelson JS (2000) Phase-resolved optical coherence tomography and optical Doppler tomography for imaging blood flow in human skin with fast scanning speed and high velocity sensitivity. Opt Lett 25(2):114–116
124. Treu CM, Lupi O, Bottino DA, Bouskela E (2011) Sidestream dark field imaging: the evolution of real-time visualization of cutaneous microcirculation and its potential application in dermatology. Arch Dermatol Res 303:69–78